TITLE:

Perivascular leukocyte clusters are essential for efficient activation of effector T cells in the skin.

AUTHOR(S):

Natsuaki, Yohei; Egawa, Gyohei; Nakamizo, Satoshi; Ono, Sachiko; Hanakawa, Sho; Okada, Takaharu; Kusuba, Nobuhiro; ... Guttman-Yassky, Emma; Miyachi, Yoshiki; Kabashima, Kenji

CITATION:

Natsuaki, Yohei ...[et al]. Perivascular leukocyte clusters are essential for efficient activation of effector T cells in the skin.. Nature immunology 2014, 15: 1064-1069

ISSUE DATE:

2014-09-21

URL:

http://hdl.handle.net/2433/189891

RIGHT:

© 2014 Nature America, Inc.; 許諾条件により本文は2015-03-22に公開.; This is not the published version. Please cite only the published version.; この論文は出版社版でありません。引用の際には出版社版をご確認ご利用ください。

京都大学学術情報リポジトリ
KURENAI 紅
Kyoto University Research Information Repository

A Self-archived copy in
Kyoto University Research Information Repository
https://repository.kulib.kyoto-u.ac.jp

1 **Perivascular leukocyte clusters are essential for efficient effector T cell activation in the**
2 **skin**
3

4 Yohei Natsuaki[1,13,15], Gyohei Egawa[1,15], Satoshi Nakamizo[1], Sachiko Ono[1], Sho Hanakawa[1],
5 Takaharu Okada[2], Nobuhiro Kusuba[1], Atsushi Otsuka[1], Akihiko Kitoh[1], Tetsuya Honda[1],
6 Saeko Nakajima[1], Soken Tsuchiya[3], Yukihiko Sugimoto[3], Ken J. Ishii[4,5], Hiroko Tsutsui[6],
7 Hideo Yagita[7], Yoichiro Iwakura[8,9], Masato Kubo[10,11], Lai guan Ng[12], Takashi Hashimoto[13],
8 Judilyn Fuentes[14], Emma Guttman-Yassky[14], Yoshiki Miyachi[1], and Kenji Kabashima[1]
9
10
11 [1] Department of Dermatology, Kyoto University Graduate School of Medicine, Kyoto, Japan.
12 [2] Research Unit for Immunodynamics, RIKEN Research Center for Allergy and Immunology,
13 Kanagawa, Japan.
14 [3] Department of Pharmaceutical Biochemistry, Graduate School of Pharmaceutical Sciences,
15 Kumamoto University, Kumamoto, Japan.
16 [4] Laboratory of Adjuvant Innovation, National Institute of Biomedical Innovation, Osaka,
17 Japan.
18 [5] Laboratory of Vaccine Science, WPI Immunology Frontier Research Center (iFReC), Osaka
19 University, Osaka, Japan.
20 [6] Departments of Microbiology, Hyogo College of Medicine, Hyogo, Japan.
21 [7] Department of Immunology, Juntendo University School of Medicine, Tokyo, Japan.
22 [8] Research Institute for Biomedical Sciences, Tokyo University of Science, Chiba, Japan
23 [9] Medical Mycology Research Center, Chiba University, Chiba, Japan
24 [10] Laboratory for Cytokine Regulation, RIKEN center for Integrative Medical Science (IMS),
25 Kanagawa, Japan.
26 [11] Division of Molecular Pathology, Research Institute for Biomedical Science, Tokyo
27 University of Science, Chiba, Japan
28 [12] Singapore Immunology Network (SIgN), A*STAR (Agency for Science, Technology and
29 Research), Biopolis, Singapore
30 [13] Department of Dermatology, Kurume University School of Medicine, Fukuoka, Japan.
31 [14] Department of Dermatology, Icahn School of Medicine at Mount Sinai School Medical
32 Center, New York, NY.
33 [15] These authors contributed equally to this work.
34

A Self-archived copy in
Kyoto University Research Information Repository
https://repository.kulib.kyoto-u.ac.jp

35 Correspondence to Kenji Kabashima, MD, PhD
36 Department of Dermatology, Kyoto University Graduate School of Medicine
37 54 Shogoin-Kawahara, Kyoto 606-8507, Japan
38 Phone: +81-75-751-3605; Fax: +81-75-761-3002
39 E-mail: kaba@kuhp.kyoto-u.ac.jp

40

京都大学 KYOTO UNIVERSITY
A Self-archived copy in
Kyoto University Research Information Repository
https://repository.kulib.kyoto-u.ac.jp
京都大学学術情報リポジトリ KURENAI 紅 Kyoto University Research Information Repository

41 It remains largely unclear how antigen-presenting cells encounter effector or memory T cells
42 efficiently in the periphery. Here we used a murine contact hypersensitivity model and
43 showed that upon epicutaneous antigen challenge, dendritic cells (DCs) formed clusters with
44 effector T cells in dermal perivascular areas to promote *in situ* proliferation and activation of
45 skin T cells in an antigen- and integrin LFA-1-dependent manner. We found that DCs
46 accumulated in perivascular areas and DC clustering was abrogated by macrophage-depletion.
47 Interleukin 1α (IL-1α) treatment induced the production of the chemokine CXCL2 from
48 dermal macrophages, and DC clustering was suppressed by blockade of either IL-1 receptor
49 (IL-1R) or CXCR2, the receptor for CXCL2. These findings suggest that dermal leukocyte
50 cluster is an essential structure for elicitation of the acquired cutaneous immunity.
51

京都大学 KYOTO UNIVERSITY
A Self-archived copy in
Kyoto University Research Information Repository
https://repository.kulib.kyoto-u.ac.jp
京都大学学術情報リポジトリ KURENAI 紅 Kyoto University Research Information Repository

52 Boundary tissues, including the skin, are continually exposed to foreign antigens, which must
53 be monitored and possibly eliminated. Upon foreign antigen exposure, skin dendritic cells
54 (DCs), including epidermal Langerhans cells (LCs), capture the antigens and migrate to
55 draining lymph nodes (LNs) where antigen presentation to naïve T cells occurs mainly in the
56 T cell zone. In this location naïve T cells accumulation in the vicinity of DCs is mediated by
57 CCR7 signaling[1]. The T cell zone in the draining LNs facilitates the efficient encounter of
58 antigen-bearing DCs with antigen-specific naïve T cells.
59 As opposed to LNs, the majority of skin T cells, including infiltrating skin T cells and skin
60 resident T cells, have an effector-memory phenotype[2]. In addition, antigen presentation to
61 skin T cells by antigen-presenting cells (APCs) is the crucial step in elicitation of acquired
62 skin immune responses, such as contact dermatitis. Therefore, we hypothesize that
63 antigen-presentation in the skin should be substantially different from that in LNs. ,Previous
64 studies using murine contact hypersensitivity (CHS), as a model of human contact dermatitis,
65 have revealed that dermal DCs (dDCs), but not epidermal LCs, have a pivotal role in the
66 transport and presentation of antigen to the LNs[3]. In the skin, however, it remains unclear
67 which subset of APCs presents antigens to skin T cells, and how skin T cells efficiently
68 encounter APCs. In addition, dermal macrophages are key modulators in CHS response[4], but
69 the precise mechanisms by which macrophages are involved in antigen recognition in the
70 skin have not yet been clarified. These unsolved questions prompted us to focus where skin T
71 cells recognize antigens and how skin T cells are activated in the elicitation phase of acquired
72 cutaneous immune responses, such as CHS.
73 When keratinocytes encounter foreign antigens, they immediately produce various
74 pro-inflammatory mediators such as interleukin 1(IL-1) and tumor necrosis factor (TNF) in
75 an antigen-nonspecific manner[5, 6]. IL-1 family proteins are considered important modulators
76 in CHS responses, because hapten-specific T cell activation was shown to be impaired in
77 IL-1α and IL-1β-deficient mice, but not in TNF-deficient mice[7]. IL-1α and IL-1β are
78 agonistic ligands of the IL-1 receptor (IL-1R). While IL-1α is stored in keratinocytes and
79 secreted upon exposure to nonspecific stimuli, IL-1β is produced mainly by epidermal LCs
80 and dermal mast cells in an inflammasome-dependent manner via NALP3 and caspase 1/11
81 activation. Because these pro-inflammatory mediators are crucial in the initiation of acquired
82 immune responses such as CHS, it is of great interest to understand how IL-1 modulates
83 antigen recognition by skin T cells.
84 Using a murine CHS model, here we examined how DCs and effector T cells encounter

京都大学 KYOTO UNIVERSITY
A Self-archived copy in
Kyoto University Research Information Repository
https://repository.kulib.kyoto-u.ac.jp
京都大学学術情報リポジトリ KURENAI 紅 Kyoto University Research Information Repository

85 each other efficiently in the skin. We found that upon encounter with antigenic stimuli dDCs
86 formed clusters in which effector T cells were activated and proliferated in an
87 antigen-dependent manner. These DC–T cell clusters were initiated by skin macrophages via
88 IL-1R signaling and were essential for the establishment of cutaneous acquired immune
89 responses.
90
91

92 **RESULTS**

93 **DC–T cell clusters are formed at antigen-challenged sites**

94 To explore immune cell accumulation in the skin, we examined the clinical and histological
95 features of elicitation of human allergic contact dermatitis. Allergic contact dermatitis is the
96 most common of eczematous skin diseases, affecting 15–20% of the general population
97 worldwide[8], and is mediated by T cells. Although antigens may be applied relatively evenly
98 over the surface of skin, clinical manifestations commonly include discretely distributed
99 small vesicles (**Fig. 1a**), suggesting an uneven occurrence of intense inflammation.
100 Histological examination of allergic contact dermatitis showed spongiosis, intercellular
101 edema in the epidermis and co-localization of perivascular infiltrates of CD3$^+$ T cells and
102 spotty accumulation of CD11c$^+$ DCs in the dermis, especially beneath the vesicles (**Fig. 1b**).
103 These findings led us to hypothesize that focal accumulation of T cells and DCs in the dermis
104 may contribute to vesicle formation in early eczema.

105 To characterize the DC–T cell clusters in elicitation reactions, we obtained time-lapse
106 images in a murine model of CHS using two-photon microscopy. T cells were isolated from
107 the draining LNs of 2, 4-dinitrofluorobenzene (DNFB)-sensitized mice, labeled and
108 transferred into CD11c-yellow fluorescent protein (YFP) mice. In the steady state, YFP$^+$
109 dDCs distributed diffusely (**Fig. 1c**), representing nondirected movement in a random fashion,
110 as reported previously (**Supplementary Fig. 1**). After topical challenge with DNFB, YFP$^+$
111 dDCs transiently increased their velocities and formed clusters in the dermis, with the clusters
112 becoming larger and more evident after 24 h (**Fig. 1c** and **Supplementary Movie 1**). At the
113 same time, transferred T cells accumulated in the DC clusters and interacted with YFP$^+$ DCs
114 for several hours (**Fig. 1d** and **Supplementary Movie 2**). Thus, the accumulation of DCs and
115 T cells in the dermis is observed in mice during CHS responses. We observed that the
116 intercellular spaces between keratinocytes overlying the DC–T cell clusters in the dermis
117 were enlarged (**Fig. 1e**), replicating observations in human allergic contact dermatitis (**Fig.
118 1b**).

京都大学 KYOTO UNIVERSITY
A Self-archived copy in
Kyoto University Research Information Repository
https://repository.kulib.kyoto-u.ac.jp
京都大学学術情報リポジトリ KURENAI 紅 Kyoto University Research Information Repository

119 We next sought to determine which of the two major DC populations in skin, epidermal LCs
120 or dDCs, were essential for the elicitation of CHS. To deplete all cutaneous DC subsets,
121 Langerin-diphtheria toxin receptor (DTR) mice were transferred with bone marrow (BM)
122 cells from CD11c-DTR mice. To selectively deplete LCs or dDCs, Langerin-DTR or
123 C57BL/6 mice were transferred with BM cells from C57BL/6 mice or CD11c-DTR mice,
124 respectively (**Supplementary Fig. 2a, b**). We injected diphtheria toxin (DT) for depletion of
125 each DC subset before elicitation and found that ear swelling and inflammatory histological
126 findings were significantly attenuated in the absence of dDCs, but not in the absence of LCs
127 (**Fig. 1f** and **Supplementary Fig. 2c**). In addition, interferon (IFN)-γ production in skin T
128 cells was strongly suppressed in dDC-depleted mice (**Fig. 1g**). These results suggest that
129 dDCs, and not epidermal LCs, are essential for T cell activation and the elicitation of CHS
130 responses.
131

132 **Skin effector T cells proliferate *in situ* in an antigen-dependent manner**

133 To evaluate the impact of DC–T cell clusters in the dermis, we determined whether T cells
134 had acquired the ability to proliferate via DC–T cell accumulation in the dermis. $CD4^+$ or
135 $CD8^+$ T cells purified from the draining LNs of DNFB-sensitized mice were labeled with
136 CellTrace^{TM} Violet and transferred into naïve mice. Twenty-four hours after DNFB
137 application, we collected the skin to evaluate T cell proliferation by dilution of fluorescent
138 intensity. The majority of infiltrating T cells were $CD44^+$ $CD62L^-$ effector T cells
139 (**Supplementary Fig. 2d**). Among the infiltrating T cells, $CD8^+$ T cells proliferated actively,
140 whereas the $CD4^+$ T cells showed low proliferative potency (**Fig. 2a**). This T cell
141 proliferation was antigen-dependent, because 2,4,6-trinitrochlorobenzene (TNCB)-sensitized
142 T cells exhibited low proliferative activities in response to DNFB application (**Fig. 2a**). In
143 line with this finding, the DC–T cell conjugation time was prolonged in the presence of
144 cognate antigens (**Fig. 2b**), and the T cells interacting with DCs within DC–T cell clusters
145 proliferated (**Fig. 2c and Supplementary Movie 3**). Our findings indicate that skin effector T
146 cells conjugate with DCs and proliferate *in situ* in an antigen-dependent manner.
147

148 **$CD8^+$ T cell activation in DC–T cell clusters is LFA-1 dependent**

149 A sustained interaction between DCs and naïve T cells, which is known as an immunological
150 synapse, is maintained by cell adhesion molecules[9]. Particularly, the integrin LFA-1 on T
151 cells binds to cell surface glycoproteins, such as intercellular adhesion molecule-1 (ICAM-1),

京都大学 KYOTO UNIVERSITY
A Self-archived copy in
Kyoto University Research Information Repository
https://repository.kulib.kyoto-u.ac.jp
京都大学学術情報リポジトリ KURENAI 紅 Kyoto University Research Information Repository

152 on APCs, which is essential for naïve T cell proliferation and activation during antigen
153 recognition in the LNs. To examine whether LFA-1-ICAM-1 interactions are required for
154 effector T cell activation in DC–T cell clusters in the skin, an anti-LFA-1 neutralizing
155 antibody, KBA, was intravenously injected 14 h after elicitation with DNFB in CHS. KBA
156 administration reduced T cells accumulation in the dermis (**Fig. 3a**). The velocity of T cells in
157 the cluster was 0.65 ± 0.29 μm/min 14 h after DNFB challenge and increased up to 3-fold
158 (1.64± 1.54 μm/min) at 8 h after treatment with KBA, while it was not affected by treatment
159 with an isotype-matched control IgG (**Fig. 3b**). At the outside of clusters, T cells smoothly
160 migrated at the mean velocity of 2.95 ± 1.19 μm/min, consistent with previous results[10], and
161 was not affected by control-IgG treatment (data not shown). Treatment with KBA also
162 attenuated ear swelling significantly (**Fig. 3c**), as well as IFN-γ production by skin $CD8^+$ T
163 cells (**Fig. 3d, e**). These results suggest that DC–effector T cell conjugates are
164 integrin-dependent, similar to the DC–naïve T cell interactions in draining LNs.
165

166 **Skin macrophages are required for dDC clustering**

167 We next examined the initiation factors of DC–T cell accumulation. dDC clusters were also
168 formed in response to the initial application of hapten (sensitization phase), but their number
169 was significantly decreased 48 h after sensitization, while DC clusters persisted for 48 h in
170 the elicitation phase (**Fig. 4a and Supplementary Fig. 3a**). These DC clusters were
171 abrogated 7 days after DNFB application (data not shown). These observations suggest that
172 DC–T cell accumulation is initiated by DC clustering, which then induces the accumulation,
173 proliferation and activation of T cells, a process that depends on the presence of
174 antigen-specific effector T cells *in situ*. DC clusters were also induced by solvents such as
175 acetone or adjuvants such as dibutylphthalic acid and *Mycobacterium bovis BCG*-inoculation
176 (**Supplementary Fig. 3b, c**). In addition, DC clusters were observed not only in the ear skin,
177 but also in other regions such as the back skin and the footpad (**Supplementary Fig. 3d**).
178 These results suggest that DC cluster formation is not an ear-specific event, but a general
179 mechanism during skin inflammation.

180 The initial DC clusters were not decreased in recombination activating gene 2
181 (RAG2)-deficient mice, in which T and B cells are absent, in lymphoid tissue inducer
182 cell-deficient *aly/aly* mice [11] or in mast cell or basophil-depleted mice, using MasTRECK or
183 BasTRECK mice[12, 13] (**Fig. 4b**). In contrast, DC clusters were abrogated in C57BL/6 mice
184 transferred with BM from LysM-DTR mice, in which both macrophages and neutrophils

京都大学 KYOTO UNIVERSITY
A Self-archived copy in
Kyoto University Research Information Repository
https://repository.kulib.kyoto-u.ac.jp
京都大学学術情報リポジトリ KURENAI 紅 Kyoto University Research Information Repository

185 were depleted by treatment with DT (**Fig. 4b, c**). The depletion of neutrophils alone, by
186 administration of anti-Ly6G antibody (1A8), did not interfere with DC cluster formation (**Fig.**
187 **4b**), which suggested that macrophages, but not neutrophils, were required during the
188 formation of DC clusters. Of note, DC cluster formation was not attenuated by anti-LFA-1
189 neutralizing KBA antibody treatment (**Supplementary Fig. 3e, f**), suggesting that
190 macrophages-DCs interaction were LFA-1-independent. Consistent with the DC cluster
191 formation, the elicitation of the CHS response (**Fig. 4d**) and IFN-γ production by skin T cells
192 (**Fig. 4e**) were significantly suppressed in LysM-DTR BM chimeric mice treated with DT.
193 Thus, skin macrophages were required for formation of DC clusters, which was necessary for
194 T cell activation and the elicitation of CHS.
195
196 **Macrophages are required for perivascular DCs clustering**
197 To examine the kinetics of dermal macrophage and DCs *in vivo*, we visualized them by
198 two-photon microscopy. *In vivo* labeling of blood vessels with tetramethylrhodamine
199 isothiocyanate (TRITC)-conjugated dextran revealed that dDCs distributed diffusely in the
200 steady state (**Fig. 5a, left**). After hapten-application to the ear of previously sensitized mice,
201 dDCs accumulated mainly around post-capillary venules (**Fig. 5a, right** and **Fig. 5b**).
202 Time-lapse imaging revealed that some of dDCs showed directional migration toward
203 TRITC-positive cells that were labeled red by incorporating extravasated TRITC-dextran
204 (**Fig. 5c and Supplementary Movie 4**). The majority of TRITC-positive cells were F4/80^{+}
205 CD11b^{+} macrophages (**Supplementary Fig. 4a**). These observations prompted us to examine
206 the role of macrophages in DC accumulation. We used a chemotaxis assay to determine
207 whether macrophages attracted the DCs. dDCs and dermal macrophages were isolated from
208 dermal skin cell suspensions and incubated in a transwell assay for 12 h. dDCs placed in the
209 upper wells efficiently migrated to the lower wells that contain dermal macrophages (**Fig. 5d**).
210 But this dDC migration was not observed when macrophages were absent in the lower wells
211 (**Fig. 5d**). Thus, dermal macrophages have a capacity to attract dDCs in vitro, which may
212 lead to dDC accumulation around post-capillary venules.
213
214 **IL-1α is required for DC cluster formation upon antigen challenge**
215 We attempted to explore the underlying mechanism of DC cluster formation. We observed
216 that DC accumulation occurred during the first application of hapten (**Fig. 4a**), which
217 suggested that an antigen-nonspecific mechanism, such as production of the

A Self-archived copy in
Kyoto University Research Information Repository
https://repository.kulib.kyoto-u.ac.jp

218 pro-inflammatory mediator IL-1, may initiate DC clustering. Hapten-induced DC
219 accumulation was not decreased in NALP3- or caspase-1-11-deficient mice, but was
220 decreased significantly in IL-1R1-deficient mice, which lack a receptor for IL-1α, IL-1β, and
221 IL-1R antagonist, or after the subcutaneous administration of an IL-1R antagonist (**Fig. 6a,b**).
222 Consistent with these observations, the elicitation of CHS and IFN-γ production by skin T
223 cells were significantly attenuated in mice that lack both IL-1α and IL-1β (**Fig. 6c, d**). In
224 addition, the formation of dDC clusters was suppressed significantly by the subcutaneous
225 injection of an anti-IL-1α neutralizing antibody, but only marginally by an anti-IL-1β
226 neutralizing antibody (**Fig. 6b**). Because keratinocytes are known to produce IL-1α upon
227 hapten application [14], our results suggest that IL-1α has a major role in mediating the
228 formation of DC clustering.
229

230 **M2 macrophages produce CXCL2 to attract dDCs**

231 To further characterize how macrophages attract dDCs, we examined *Il1r1* expression in
232 BM-derived M1 and M2 macrophages, classified as such based on the differential mRNA
233 expression of *Tnf, Nos2*, *Il12a*, *Arg1*, *Retnla* and *Chi313* (**Supplementary Fig. 4b**) [15]. We
234 found that M2 macrophages had higher expression of *Il1r1* mRNA compared to M1
235 macrophages (**Fig. 6e**). We also found that the subcutaneous injection of pertussis toxin, a
236 inhibitory regulative G protein (Gi)-specific inhibitor, almost completely abrogated DC
237 cluster formation in response to hapten-stimuli (**Fig. 6b**) suggesting that signaling through
238 Gi-coupled chemokines was required for DC cluster formation.
239 We next used microarrays to examine the effect of IL-1α on the expression of chemokines
240 in M1 and M2 macrophages. IL-1α treatment did not enhance chemokine expression in M1
241 macrophages, whereas it increased *Ccl5*, *Ccl17*, *Ccl22* and *Cxcl2* mRNA expression in M2
242 macrophages (**Supplementary Table 1**). Among them, *Cxcl2* expression was enhanced most
243 prominently by treatment with IL-1α, a result validated by real-time polymerase chain
244 reaction (PCR) analysis (**Fig. 6f**). Consistently, *Cxcl2* mRNA expression was significantly
245 increased in DNFB-painted skin (**Supplementary Fig. 5a**) and was not affected by
246 neutrophil depletion with 1A8 (**Supplementary Fig. 5b, c**). In addition, IL-1α-treated dermal
247 macrophages produced *Cxcl2* mRNA *in vitro* (**Supplementary Fig. 5d**). These results
248 suggest that dermal macrophages, but not neutrophils, are the major source of CXCL2 during
249 CHS. We also detected high expression of the mRNA for *Cxcr2*, the receptor for CXCL2, in
250 DCs (**Supplementary Fig. 5e**), which prompted us to examine the role of CXCR2 on dDCs.

京都大学 KYOTO UNIVERSITY
A Self-archived copy in
Kyoto University Research Information Repository
https://repository.kulib.kyoto-u.ac.jp
京都大学学術情報リポジトリ KURENAI 紅 Kyoto University Research Information Repository

251 The formation of DC clusters in response to hapten stimuli was substantially reduced by the
252 intraperitoneal administration of the CXCR2 inhibitor SB265610 [16] (**Fig. 6g**). In addition,
253 SB265610-treatment during the elicitation of CHS inhibited ear swelling (**Fig. 6h**) and IFN-γ
254 production by skin T cells (**Fig. 6i**).
255 Taken together, in the absence of effector T cells specific for a cognate antigen (i.e. in the
256 sensitization phase of CHS), DC clustering is a transient event, and hapten-carrying DCs
257 migrate into draining LNs to establish sensitization. On the other hand, in the presence of the
258 antigen and antigen-specific effector or memory T cells, DC clustering is followed by T cell
259 accumulation (i.e. in the elicitation phase of CHS) (**Supplementary Fig. 6**). Thus, dermal
260 macrophages are essential for initiating DC cluster formation through the production of
261 CXCL2, and that DC clustering plays an important role for efficient activation of skin T cells.
262
263
264 **DISCUSSION**
265 Although the mechanistic events in the sensitization phase in cutaneous immunity have been
266 studied thoroughly over 20 years[17, 18], what types of immunological events occur during the
267 elicitation phases in the skin has remained unclear. Here we describe the antigen-dependent
268 induction of DC and T cell clusters in the skin in a murine model of CHS and show that
269 effector T cells-DCs interactions in these clusters are required to induce efficient
270 antigen-specific immune responses in the skin. We show that dDCs, but not epidermal LCs,
271 are essential for antigen presentation to skin effector T cells and they exhibit sustained
272 association with effector T cells in an antigen- and LFA-1-dependent manner. IL-1α, and not
273 the inflammasome, initiates the formation of these perivascular DC clusters.
274 Epidermal contact with antigens triggers release of IL-1 in the skin[14]. Previous studies have
275 shown that the epidermal keratinocytes constitute a major reservoir of IL-1α[6] and mechanical
276 stress to keratinocytes permits release of large amounts of IL-1α even in the absence of cell
277 death[19]. The cellular source of IL-1α in this process remains unclear. We show that IL-1α
278 activates macrophages that subsequently attract dDCs, mainly to areas around post-capillary
279 venules, where effector T cells are known to transmigrate from the blood into the skin[20]. In
280 the presence of the antigen and antigen-specific effector T cells, DC clustering is followed by
281 T cell accumulation. Therefore, we propose that these perivascular dDC clusters may provide
282 antigen-presentation sites for efficient effector T cell activation. This is suggested by the
283 observations that CHS responses and intracutaneous T cell activation were attenuated

A Self-archived copy in
Kyoto University Research Information Repository
https://repository.kulib.kyoto-u.ac.jp

284 significantly in the absence of these clusters, in condition of macrophage depletion or
285 inhibiting integrin functions, IL-1R signaling[21, 22] or CXCR2 signaling[23].
286 In contrast to the skin, antigen presentations in other peripheral barrier tissues is relatively
287 well understood. In submucosal areas, specific sentinel lymphoid structures called
288 mucosa-associated lymphoid tissue (MALT), serve as peripheral antigen presentation sites[24],
289 and lymphoid follicles are present in the normal bronchi (bronchus-associated lymphoid
290 tissue; BALT). These structures serve as antigen presentation sites in non-lymphoid
291 peripheral organs. By analogy, the concept of skin-associated lymphoid tissue (SALT) was
292 proposed in the early 1980's, based on findings that cells in the skin are capable of capturing,
293 processing and presenting antigens[25, 26]. However, the role of cellular skin components as
294 antigen presentation sites has remained uncertain. Here we have identified an inducible
295 structure formed by dermal macrophages, dDCs and effector T cells, which seem to
296 accumulate sequentially. Because formation of this structure is essential for efficient effector
297 T cell activation, these inducible leukocyte clusters may function as SALTs. Unlike MALTs,
298 these leukocyte clusters are not found at steady state, but are induced during the development
299 of an adaptive immune response. Therefore, these clusters may be better named as inducible
300 SALTs (iSALT), similar to inducible BALTs (iBALT) in the lung[27]. In contrast to iBALTs, we
301 could not identify naïve T cells or B cells in SALTs (data not shown), suggesting that the
302 leukocyte clusters in the skin may be specialized for effector T cell activation but not for
303 naïve T cell activation. Our findings suggest that approaches to the selective inhibition of this
304 structure may have novel therapeutic benefit in inflammatory disorders of the skin.
305
306
307 **ACKNOWLEDGEMENTS**
308 We thank Dr. P. Bergstresser and Dr. J. Cyster for critical reading of our manuscript. This
309 work was supported in part by Grants-in-Aid for Scientific Research from the Ministry of
310 Education, Culture, Sports, Science and Technology of Japan.
311
312
313 **AUTHOR CONTRIBUTIONS**
314 Y.N., G.E., and K.K designed this study and wrote the manuscript. Y.N., G.E, S.N., S.O., S.H.,
315 N.K., A.O., A.K., T.H., and S.N. performed the experiments and data analysis. S.T. and Y.S.
316 did experiments related to microarray analysis. J.F. and E. G-Y did experiments related to
317 immunohistochemistry of human samples. K.J.I, H.T., H. Y, Y. I., L.G.N., and M.K.

A Self-archived copy in
Kyoto University Research Information Repository
https://repository.kulib.kyoto-u.ac.jp

318 developed experimental reagents and gene-targeted mice. T.O., Y.M., and K.K. directed the
319 project and edited the manuscript. All authors reviewed and discussed the manuscript.
320
321
322 **COMPETENG FINANCIAL INTERESTS**
323 The authors declare no competing financial interests.
324
325
326 **ACCESSION CODES**
327 Microarray data have been deposited in NCBI-GEO under accession number GSE53680.
328
329

A Self-archived copy in
Kyoto University Research Information Repository
https://repository.kulib.kyoto-u.ac.jp

330 **REFERENCES**

331 1. von Andrian UH, Mempel TR. Homing and cellular traffic in lymph nodes. *Nat Rev*
332 *Immunol* 2003, **3**(11)**:** 867-878.
333
334 2. Clark RA, Chong B, Mirchandani N, Brinster NK, Yamanaka K, Dowgiert RK*, et al.*
335 The vast majority of CLA+ T cells are resident in normal skin. *J Immunol* 2006,
336 **176**(7)**:** 4431-4439.
337
338 3. Wang L, Bursch LS, Kissenpfennig A, Malissen B, Jameson SC, Hogquist KA.
339 Langerin expressing cells promote skin immune responses under defined conditions. *J*
340 *Immunol* 2008, **180**(7)**:** 4722-4727.
341
342 4. Tuckermann JP, Kleiman A, Moriggl R, Spanbroek R, Neumann A, Illing A*, et al.*
343 Macrophages and neutrophils are the targets for immune suppression by
344 glucocorticoids in contact allergy. *J Clin Invest* 2007, **117**(5)**:** 1381-1390.
345
346 5. Sims JE, Smith DE. The IL-1 family: regulators of immunity. *Nat Rev Immunol* 2010,
347 **10**(2)**:** 89-102.
348
349 6. Murphy JE, Robert C, Kupper TS. Interleukin-1 and cutaneous inflammation: a
350 crucial link between innate and acquired immunity. *J Invest Dermatol* 2000, **114**(3)**:**
351 602-608.
352
353 7. Nakae S, Komiyama Y, Narumi S, Sudo K, Horai R, Tagawa Y*, et al.* IL-1-induced
354 tumor necrosis factor-alpha elicits inflammatory cell infiltration in the skin by
355 inducing IFN-gamma-inducible protein 10 in the elicitation phase of the contact
356 hypersensitivity response. *Int Immunol* 2003, **15**(2)**:** 251-260.
357
358 8. Thyssen JP, Linneberg A, Menne T, Nielsen NH, Johansen JD. Contact allergy to
359 allergens of the TRUE-test (panels 1 and 2) has decreased modestly in the general
360 population. *Br J Dermatol* 2009, **161**(5)**:** 1124-1129.
361
362 9. Springer TA, Dustin ML. Integrin inside-out signaling and the immunological synapse.
363 *Curr Opin Cell Biol* 2012, **24**(1)**:** 107-115.

京都大学 KYOTO UNIVERSITY
A Self-archived copy in
Kyoto University Research Information Repository
https://repository.kulib.kyoto-u.ac.jp
京都大学学術情報リポジトリ KURENAI 紅 Kyoto University Research Information Repository

364
365 10. Egawa G, Honda T, Tanizaki H, Doi H, Miyachi Y, Kabashima K. In vivo imaging of
366 T-cell motility in the elicitation phase of contact hypersensitivity using two-photon
367 microscopy. *J Invest Dermatol* 2011, **131**(4)**:** 977-979.
368
369 11. Miyawaki S, Nakamura Y, Suzuka H, Koba M, Yasumizu R, Ikehara S*, et al.* A new
370 mutation, aly, that induces a generalized lack of lymph nodes accompanied by
371 immunodeficiency in mice. *Eur J Immunol* 1994, **24**(2)**:** 429-434.
372
373 12. Sawaguchi M, Tanaka S, Nakatani Y, Harada Y, Mukai K, Matsunaga Y*, et al.* Role of
374 mast cells and basophils in IgE responses and in allergic airway hyperresponsiveness.
375 *J Immunol* 2012, **188**(4)**:** 1809-1818.
376
377 13. Otsuka A, Kubo M, Honda T, Egawa G, Nakajima S, Tanizaki H*, et al.* Requirement
378 of interaction between mast cells and skin dendritic cells to establish contact
379 hypersensitivity. *PLoS One* 2011, **6**(9)**:** e25538.
380
381 14. Enk AH, Katz SI. Early molecular events in the induction phase of contact sensitivity.
382 *Proc Natl Acad Sci U S A* 1992, **89**(4)**:** 1398-1402.
383
384 15. Weisser SB, McLarren KW, Kuroda E, Sly LM. Generation and characterization of
385 murine alternatively activated macrophages. *Methods Mol Biol* 2013, **946:** 225-239.
386
387 16. Liao L, Ning Q, Li Y, Wang W, Wang A, Wei W*, et al.* CXCR2 blockade reduces
388 radical formation in hyperoxia-exposed newborn rat lung. *Pediatr Res* 2006, **60**(3)**:**
389 299-303.
390
391 17. Honda T, Egawa G, Grabbe S, Kabashima K. Update of immune events in the murine
392 contact hypersensitivity model: toward the understanding of allergic contact
393 dermatitis. *J Invest Dermatol* 2013, **133**(2)**:** 303-315.
394
395 18. Kaplan DH, Igyarto BZ, Gaspari AA. Early immune events in the induction of allergic
396 contact dermatitis. *Nat Rev Immunol* 2012, **12**(2)**:** 114-124.
397

A Self-archived copy in
Kyoto University Research Information Repository
https://repository.kulib.kyoto-u.ac.jp

398 19. Lee RT, Briggs WH, Cheng GC, Rossiter HB, Libby P, Kupper T. Mechanical
399 deformation promotes secretion of IL-1 alpha and IL-1 receptor antagonist. *J Immunol*
400 1997, **159**(10)**:** 5084-5088.
401
402 20. Sackstein R, Falanga V, Streilein JW, Chin YH. Lymphocyte adhesion to psoriatic
403 dermal endothelium is mediated by a tissue-specific receptor/ligand interaction. *J*
404 *Invest Dermatol* 1988, **91**(5)**:** 423-428.
405
406 21. Kish DD, Gorbachev AV, Fairchild RL. IL-1 receptor signaling is required at multiple
407 stages of sensitization and elicitation of the contact hypersensitivity response. *J*
408 *Immunol* 2012, **188**(4)**:** 1761-1771.
409
410 22. Kondo S, Pastore S, Fujisawa H, Shivji GM, McKenzie RC, Dinarello CA*, et al.*
411 Interleukin-1 receptor antagonist suppresses contact hypersensitivity. *J Invest*
412 *Dermatol* 1995, **105**(3).
413
414 23. Cattani F, Gallese A, Mosca M, Buanne P, Biordi L, Francavilla S*, et al.* The role of
415 CXCR2 activity in the contact hypersensitivity response in mice. *Eur Cytokine Netw*
416 2006, **17**(1)**:** 42-48.
417
418 24. Brandtzaeg P, Kiyono H, Pabst R, Russell MW. Terminology: nomenclature of
419 mucosa-associated lymphoid tissue. *Mucosal Immunol* 2008, **1**(1)**:** 31-37.
420
421 25. Streilein JW. Skin-associated lymphoid tissues (SALT): origins and functions. *J Invest*
422 *Dermatol* 1983, 80 Suppl**:** 12s-16s.
423
424 26. Egawa G, Kabashima K. Skin as a peripheral lymphoid organ: revisiting the concept
425 of skin-associated lymphoid tissues. *J Invest Dermatol* 2011, **131**(11)**:** 2178-2185.
426
427 27. Moyron-Quiroz JE, Rangel-Moreno J, Kusser K, Hartson L, Sprague F, Goodrich S,
428 *et al.* Role of inducible bronchus associated lymphoid tissue (iBALT) in respiratory
429 immunity. *Nat med* 2004, **10**(9)**:** 927-934.
430
431 28. Kissenpfennig A, Henri S, Dubois B, Laplace-Builhe C, Perrin P, Romani N*, et al.*

京都大学 KYOTO UNIVERSITY
A Self-archived copy in
Kyoto University Research Information Repository
https://repository.kulib.kyoto-u.ac.jp
京都大学学術情報リポジトリ KURENAI 紅 Kyoto University Research Information Repository

432 Dynamics and function of Langerhans cells in vivo: dermal dendritic cells colonize
433 lymph node areas distinct from slower migrating Langerhans cells. *Immunity* 2005,
434 **22**(5)**:** 643-654.
435
436 29. Jung S, Unutmaz D, Wong P, Sano G, De los Santos K, Sparwasser T*, et al.* In vivo
437 depletion of CD11c+ dendritic cells abrogates priming of CD8+ T cells by exogenous
438 cell-associated antigens. *Immunity* 2002, **17**(2)**:** 211-220.
439
440 30. Lindquist RL, Shakhar G, Dudziak D, Wardemann H, Eisenreich T, Dustin ML*, et al.*
441 Visualizing dendritic cell networks in vivo. *Nat immunol* 2004, **5**(12)**:** 1243-1250.
442
443 31. Miyake Y, Kaise H, Isono K, Koseki H, Kohno K, Tanaka M. Protective role of
444 macrophages in noninflammatory lung injury caused by selective ablation of alveolar
445 epithelial type II Cells. *J Immunol* 2007, **178**(8)**:** 5001-5009.
446
447 32. Hao Z, Rajewsky K. Homeostasis of peripheral B cells in the absence of B cell influx
448 from the bone marrow. *J Exp Med* 2001, **194**(8)**:** 1151-1164.
449
450 33. Horai R, Asano M, Sudo K, Kanuka H, Suzuki M, Nishihara M*, et al.* Production of
451 mice deficient in genes for interleukin (IL)-1alpha, IL-1beta, IL-1alpha/beta, and IL-1
452 receptor antagonist shows that IL-1beta is crucial in turpentine-induced fever
453 development and glucocorticoid secretion. *J Exp Med* 1998, **187**(9)**:** 1463-1475.
454
455 34. Coban C, Igari Y, Yagi M, Reimer T, Koyama S, Aoshi T*, et al.* Immunogenicity of
456 whole-parasite vaccines against Plasmodium falciparum involves malarial hemozoin
457 and host TLR9. *Cell Host Microbe* 2010, **7**(1)**:** 50-61.
458
459 35. Martinon F, Petrilli V, Mayor A, Tardivel A, Tschopp J. Gout-associated uric acid
460 crystals activate the NALP3 inflammasome. *Nature* 2006, **440**(7081)**:** 237-241.
461
462 36. Koedel U, Winkler F, Angele B, Fontana A, Flavell RA, Pfister HW. Role of
463 Caspase-1 in experimental pneumococcal meningitis: Evidence from pharmacologic
464 Caspase inhibition and Caspase-1-deficient mice. *Ann Neurol* 2002, **51**(3)**:** 319-329.
465

A Self-archived copy in
Kyoto University Research Information Repository
https://repository.kulib.kyoto-u.ac.jp

466 37. Tomura M, Honda T, Tanizaki H, Otsuka A, Egawa G, Tokura Y, *et al.* Activated
467 regulatory T cells are the major T cell type emigrating from the skin during a
468 cutaneous immune response in mice. *J Clin Invest* 2010, **120**(3)**:** 883-893.

469

470

京都大学 KYOTO UNIVERSITY
A Self-archived copy in
Kyoto University Research Information Repository
https://repository.kulib.kyoto-u.ac.jp
KURENAI 紅 Kyoto University Research Information Repository

471 **METHODS**

472 **Mice**

473 Female 8- to 12-week-old C57BL/6-background mice were used in this study. C57BL/6N
474 mice were purchased from SLC (Shizuoka, Japan). Langerin-eGFP-DTR[28], CD11c-DTR[29],
475 CD11c-YFP[30], LysM-DTR[31], Rag2-deficient[32], MasTRECK[12, 13], BasTRECK [12, 13],
476 ALY/NscJcl-*aly/aly*[11], IL-1α/β-deficient[33], IL-1R1-deficient[34], NLRP3-deficient[35], and
477 caspase-1/11-deficient mice[36] were described previously. All experimental procedures were
478 approved by the Institutional Animal Care and Use Committee of Kyoto University Graduate
479 School of Medicine.

480

481 **Human Subjects**

482 Human skin biopsy samples were obtained from a nickel-reactive patch after 48 h from
483 placement of nickel patch tests in patients with a previously proven allergic contact dermatitis.
484 A biopsy of petrolatum-occluded skin was also obtained as a control. Informed consent was
485 obtained under IRB approved protocols at the Icahn School of Medicine at Mount Sinai
486 School Medical Center, and the Rockefeller University in New York.

487

488 **Induction of contact hypersensitivity (CHS) response**

489 Mice were sensitized on shaved abdominal skin with 25 μl 0.5% (w/v)
490 1-fluoro-2,4-dinitrofluorobenzene (DNFB; Nacalai Tesque, Kyoto, Japan) dissolved in
491 acetone/olive oil (4/1). Five days later, the ears were challenged with 20 μl 0.3% DNFB. For
492 adoptive transfer, T cells were magnetically sorted using auto MACS (Miltenyi Biotec,
493 Bergisch Gladbach, Germany) from the draining LNs of sensitized mice and then transferred
494 1x 10^7 cells intravenously into naïve mice.

495

496 **Depletion of cutaneous DC subsets, macrophages, and neutrophils**

497 To deplete all cutaneous DC subsets (including LCs), 6-week-old Langerin-DTR mice were
498 irradiated (two doses of 550 Rad given 3 h apart) and were transferred with 1 x 10^7 BM cells
499 from CD11c-DTR mice. Eight weeks later, 2 μg diphtheria toxin (DT; Sigma-Aldrich, St.
500 Louis, MO) was intraperitoneally injected. To selectively deplete LCs, irradiated
501 Langerin-DTR mice were transferred with BM cells from C57BL/6 mice, and 1 μg DT was
502 injected. To selectively deplete dermal DCs, irradiated C57BL/6 mice were transferred with
503 BM cells from CD11c-DTR mice, and 2 μg DT was injected. For macrophage depletion,

A Self-archived copy in
Kyoto University Research Information Repository
https://repository.kulib.kyoto-u.ac.jp

504 irradiated C57BL/6 mice were transferred with BM cells from LysM-DTR mice and 800 ng
505 DT was injected. For neutrophil depletion, 0.5 mg/body anti-Ly6G antibody (1A8, BioXCell,
506 Shiga, Japan) were intravenously administered to mice 24 h before experiment.
507

508 **Time-lapse imaging of cutaneous DCs, macrophages, and T cells**

509 Cutaneous DCs were observed using CD11c-YFP mice. To label cutaneous macrophages *in*
510 *vivo*, 5 mg TRITC-dextran (Sigma-Aldrich) was intravenously injected and mice were left for
511 24 h. At that time, cutaneous macrophages become fluorescent because they incorporated
512 extravasated dextran. To label skin-infiltrating T cells, T cells from DNFB-sensitized mice
513 were labeled with CellTracker Orange CMTMR (Invitrogen, Carlsbad, CA) and adoptively
514 transferred. Keratinocytes and sebaceous glands were visualized with the subcutaneous
515 injection of isolectin B4 (Invitrogen) and BODIPY (Molecular Probes, Carlsbad, CA),
516 respectively. Mice were positioned on the heating plate on the stage of a two-photon
517 microscope IX-81 (Olympus, Tokyo, Japan) and their ear lobes were fixed beneath a cover
518 slip with a single drop of immersion oil. Stacks of 10 images, spaced 3 μm apart, were
519 acquired at 1 to 7 min intervals for up to 24 h. To calculate T cell and DC velocities, movies
520 from 3 independent mice were processed and analyzed using Imaris7.2.1 (Bitplane, South
521 Windsor, CT) for each experiment.
522

523 **Histology and immunohistochemistry**

524 For histological examination, tissues were fixed with 10% formalin in phosphate buffer saline,
525 and then embedded in paraffin. Sections with a thickness of 5 μm were prepared and
526 subjected to staining with hematoxylin and eosin. For whole-mount staining, the ears were
527 split into dorsal and ventral halves, and incubated with 0.5 M ammonium thiocyanate for 30
528 min at 37°C [37]. Then the dermal sheets were separated and fixed in acetone for 10 min at
529 -20°C. After treatment with Image-iT FX Signal Enhancer (Invitrogen), the sheets were
530 incubated with anti-mouse MHC class II antibody (eBioscience, San Diego, CA) followed by
531 incubation with secondary antibody conjugated to Alexa 488 or 594 (Invitrogen). The slides
532 were mounted using a ProLong Antifade kit with DAPI (Molecular Probes) and observed
533 under a fluorescent microscope (BZ-900, KEYENCE, Osaka, Japan). The number/size of DC
534 clusters were evaluated in 10 fields of 1mm^2/ ear and were scored according to the criteria
535 shown in Supplementary Fig. 5a.
536

京都大学 KYOTO UNIVERSITY
A Self-archived copy in
Kyoto University Research Information Repository
https://repository.kulib.kyoto-u.ac.jp
京都大学学術情報リポジトリ KURENAI 紅 Kyoto University Research Information Repository

537

538 **Cell isolation and flow cytometry**

539 To isolate skin lymphocytes, the ear splits were put into digestion buffer
540 (RPMI supplemented with 2% fetal calf serum, 0.33 mg/ml of Liberase TL (Roche, Lewes,
541 UK), and 0.05% DNase I (Sigma-Aldrich)) for 1 hr at 37°C. After the incubation, the tissue
542 was disrupted by passage through a 70 µm cell strainer and stained with respective antibodies.
543 For analysis of intracellular cytokine production, cell suspensions were obtained in the
544 presence of 10 µg/ml of Brefeldine A (Sigma-Aldrich) and were fixed with Cytofix buffer,
545 permeabilized with Perm/Wash buffer (BD Biosciences) as per the manufacturer's protocol.
546 To stain cells, anti-mouse CD4, CD8, CD11b, CD11c, B220, MHC class II, F4/80, IFN-γ,
547 Gr1 antibodies and 7-amino-actinomycin D (7AAD) were purchased from eBioscience.
548 Anti-mouse CD45 antibody (BioLegend, San Diego, CA), anti-TCR-β antibody (BioLegend),
549 and anti-CD16/CD32 antibody (BD Biosciences) were purchased. Flow cytometry was
550 performed using LSRFortessa (BD Biosciences) and analyzed with FlowJo (TreeStar, San
551 Carlos, CA).

552

553 **Chemotaxis assay**

554 Chemotaxis was performed as described previously with some modifications [37]. In brief, the
555 dermis of the ear skin was minced and digested with 2 mg/ml collagenase type II
556 (Worthington Biochemical, NY) containing 1 mg/ml hyaluronidase (Sigma-Aldrich) and 100
557 µg/ml DNase I (Sigma-Aldrich) for 30 min at 37°C. DDCs and macrophages were isolated
558 using auto-MACS. Alternatively, BM-derived DCs and macrophages were prepared. 1 x 10^6
559 DCs were added to the 5 µm pore-size transwell insert (Corning, Cambridge, MA) and 5 x
560 10^5 macrophages were added into the lower wells, and the cells were incubated at 37°C for
561 12 h. A known number of fluorescent reference beads (FlowCount fluorospheres, Beckman
562 Coulter, Fullerton, CA) were added to each sample to allow accurate quantification of
563 migrated cells in the lower wells by flow cytometry.

564

565 **Cell proliferation assay with CellTrace™ Violet**

566 Mice were sensitized with 25 µl 0.5% DNFB or 7% trinitrochlorobenzene (Chemical Industry,
567 Tokyo, Japan). Five days later, T cells were magnetically separated from the draining LNs of
568 each group, and labeled with CellTrace™ Violet (Invitrogen) as per the manufacturer's
569 protocol. Ten million T cells were adoptively transferred to naïve mice, and the ears were

京都大学 KYOTO UNIVERSITY
A Self-archived copy in
Kyoto University Research Information Repository
https://repository.kulib.kyoto-u.ac.jp
京都大学学術情報リポジトリ KURENAI 紅 Kyoto University Research Information Repository

570 challenged with 20 μl of 0.5% DNFB. Twenty-four hours later, ears were collected and
571 analyzed by flow cytometry.
572

573 **In vitro differentiation of DCs, M1 and M2-phenotype macrophages from BM cells**

574 BM cells from the tibias and fibulas were plated 5×10^6 cells/ 10cm dishes on day 0. For DC
575 differentiation, cells were cultured at 37°C in 5% CO_2 in cRPMI medium
576 (RPMI supplemented with 1% L-glutamine, 1% Hepes, 0.1% 2ME and 10% fetal bovine
577 serum) containing 10 ng/mL GM-CSF (Peprotech, Rocky Hill, NJ). For macrophages
578 differentiation, BM cells were cultured in cRPMI containing 10 ng/mL M-CSF (Peprotech).
579 Medium was replaced on days 3 and 6 and cells were harvested on day 9. To induce M1 or
580 M2 phenotypes, cells were stimulated for 48 h with IFN-γ (10 ng/mL; R&D Systems,
581 Minneapolis, MN) or with IL-4 (20 ng/mL; R&D Systems), respectively.
582

583 **In vitro IL-1α stimulation assay of dermal macrophages**

584 Dermal macrophages were separated from IL-1α/β-deficient mice[33] to avoid pre-activation
585 during cell preparations. Ear splits were treated with 0.25% trypsin/EDTA for 30 min at 37°C
586 to remove epidermis and then minced and incubated with collagenase as previously described.
587 $CD11b^+$ cells were separated using MACS and 2×10^5 cells/well were incubated with or
588 without 10 ng/ml IL-1α (R&D systems) in 96-well plate for 24 h.
589

590 **Blocking assay**

591 For LFA-1 blocking assay, mice were intravenously injected with 100 μg anti-LFA-1
592 neutralizing antibody, KBA, 12-14 h after challenge with 20 μl 0.5% DNFB. For IL-1R
593 blocking, mice were subcutaneously injected with 10 μg IL-1R antagonist (PROSPEC, East
594 Brunswick, NJ) 5 h before challenge. For blocking of CXCR2, mice were intraperitoneally
595 treated with 50 μg CXCR2 inhibitor SB265610[16] (Tocris Bioscience, Bristol, UK) 6 h before
596 and at hapten painting.
597

598 **Quantitative PCR analysis**

599 Total RNA was isolated using an RNeasy Mini kit (Qiagen, Hilden, Germany). cDNA was
600 synthesized using a PrimeScript RT reagent kit (TaKaRa, Ohtsu, Japan) with random
601 hexamers as per the manufacturer's protocol. Quantitative PCR was carried out with a
602 LightCycler 480 using a LightCycler SYBR Green I master (Roche) as per the

京都大学 KYOTO UNIVERSITY
A Self-archived copy in
Kyoto University Research Information Repository
https://repository.kulib.kyoto-u.ac.jp
京都大学学術情報リポジトリ KURENAI 紅 Kyoto University Research Information Repository

603 manufacturer's protocol. The relative expression of each gene was normalized against that of
604 Gapdh. Primer sequences are shown in Supplementary Table 2.
605
606 **Microarray analysis**
607 Total RNA was isolated using the RNeasy Mini Kit (Qiagen) as per the manufacturers'
608 protocol. An amplified sense-strand DNA product was synthesized by the Ambion WT
609 Expression Kit (Life Technologies, Gaithersburg, MD), and was fragmented and labeled by
610 the WT Terminal Labeling and Controls Kit (Affymetrix, Santa Clara, CA), and was
611 hybridized to the Mouse Gene 1.0 ST Array (Affymetrix). We used the robust multi-array
612 average algorithm for log transformation (log2) and normalization of the GeneChip data.
613 Microarray data have been deposited in NCBI-GEO under accession number GSE53680.
614
615 **General experimental design and statistical analysis**
616 For animal experiments, a sample size of three to five mice per group was determined on the
617 basis of past experience in generating statistical significance. Mice were randomly assigned
618 to study groups and no specific randomization or blinding protocol was used. Sample or
619 mouse identity was not masked for any of these studies. Statistical analyses were performed
620 using Prism software (GraphPad Software Inc.). Normal distribution was assumed a priori for
621 all samples. Unless indicated otherwise, an unpaired parametric *t*-test was used for
622 comparison of data sets. In cases in which the data point distribution was not Gaussian, a
623 nonparametric *t*-test was also applied. *P* values of less than 0.05 were considered significant.
624
625
626

京都大学 KYOTO UNIVERSITY
A Self-archived copy in
Kyoto University Research Information Repository
https://repository.kulib.kyoto-u.ac.jp
京都大学学術情報リポジトリ KURENAI 紅 Kyoto University Research Information Repository

627 **Figure Legends**

628 **Figure 1:** DC–T cell cluster formation is responsible for epidermal eczematous conditions.
629 (**a**) Clinical manifestations of allergic contact dermatitis in human skin 48 h after a patch test
630 with nickel. Scale bar = 200 μm. (**b**) Hematoxylin and eosin, anti-CD3, and anti-CD11c
631 staining of the human skin biopsy sample from an eczematous legion. Asterisks and
632 arrowheads denote epidermal vesicles and dDC–T cell clusters, respectively. Scale bar = 250
633 μm. (**c**) Sequential images of leukocyte clusters in the elicitation phase of CHS. White circles
634 represent DC (green) and T cell (red) dermal accumulations. Scale bar = 100 μm. (**d**) A high
635 magnification view of DC–T cell cluster in Fig.1c. Scale bar = 10 μm. (**e**) Intercellular edema
636 of the epidermis overlying DC–T cell cluster in the dermis. Keratinocytes (red) are visualized
637 with isolectin B4. The right panel shows the mean distance between adjacent keratinocytes
638 above (+) or not above (-) DC–T cell cluster (n=20, each). Scale bar = 10 μm. (**f**) Ear
639 swelling 24 h after CHS in subset-specific DC-depletion models (n = 5, each). *, $P < 0.001$.
640 (**g**) The number (left) and the % frequency (right) of IFN-γ producing T cells in the ear 18 h
641 after CHS with or without dDC-depletion (n = 5, each). *, $P < 0.05$.
642

643 **Figure 2:** Antigen-dependent T cell proliferation in DC–T cell clusters. (**a**) T cell
644 proliferation in the skin. $CD4^+$ and $CD8^+$ T cells from DNFB- (red) or TNCB- (blue)
645 sensitized mice were labeled with CellTrace™ Violet and transferred. The dilutions of tracer
646 in the challenged sites were examined 24 h later. (**b**) Conjugation time of DNFB- (red, n =
647 160) or TNCB-sensitized (blue, n = 60) T cells with dDCs 24 h after DNFB challenge. *, $P <$
648 0.05. (**c**) Sequential images of dividing T cells (red) in DC–T cell clusters. Green represents
649 dDCs. Arrowheads represent a dividing T cell.
650

651 **Figure 3:** LFA-1 is essential for the persistence of DC–T cell clustering and for T cell
652 activation in the skin. (**a**) DC (green) and T cell (red) clusters in the DNFB-challenged site
653 before (0 h) and 9 h after KBA or isotype-matched IgG treatment. Scale bar = 100 μm. (**b**)
654 Fold changes of T cell velocities in DNFB-challenged sites after KBA or control IgG
655 treatment (n = 30, each). (**c**) Ear swelling 24 h after KBA (red) or control IgG (black)
656 treatment with DNFB challenge (n = 5, each). (**d** and **e**) IFN-γ production by $CD8^+$ T cells (d)
657 and the number of IFN-γ producing cells in $CD4^+$ or $CD8^+$ populations (e) in KBA (red) or
658 control IgG (black) treated mice (n = 5, each). DNFB-sensitized mice were treated with KBA
659 or control IgG 12 h after DNFB challenge and the skin samples were obtained 6 h later. *, *P*

京都大学 KYOTO UNIVERSITY
A Self-archived copy in
Kyoto University Research Information Repository
https://repository.kulib.kyoto-u.ac.jp
京都大学学術情報リポジトリ KURENAI 紅 Kyoto University Research Information Repository

660 < 0.05.

661

662 **Figure 4:** Macrophages are essential for DC cluster formation. (**a**) Score of DC cluster
663 number 24 h and 48 h after DNFB application in sensitization (red) or elicitation (green)
664 phase of CHS (n=4, each). (**b**) Score of DC cluster number in non-treated (NT) mice and
665 DNFB-applicated-C57BL/6 (WT), Rag2-deficient, aly/aly, MasTRECK, BasTRECK,
666 LysM-DTR, and 1A8-treated mice (n=4, each). *, $P < 0.05$. (**c**) DC clusters observed in
667 LysM-DTR BM chimeric mice with or without DT-treatment. Scale bar = 100 μm. (**d**) Ear
668 swelling 24 h after DNFB application in LysM-DTR BM chimeric mice with (red) or without
669 (black) DT-treatment (n = 5, each). (**e**) The number (left) and the % frequency (right) of
670 IFN-γ producing $CD8^+$ T cells in the ear 18 h after DNFB application in LysM-DTR BM
671 chimeric mice with (red) or without (black) DT-treatment (n = 5, each). *, $P < 0.05$.

672

673 **Figure 5**: Macrophages mediate perivascular DC cluster formation. (**a**) A distribution of
674 dDCs (green) in the steady state (left) and in the elicitation phase of CHS (right). The white
675 circles show DC clusters. Sebaceous glands visualized with BODIPY (green) are indicated by
676 arrows. Blood vessels, yellow/red; macrophages, red. (**b**) A high magnification view of
677 perivascular DC cluster. Scale bar = 100 μm.(**c**) Sequential images of dDCs (green) and
678 macrophages (red) in the elicitation phase of CHS. The white dashed line represents the track
679 of a DC. (**d**) Chemotaxis assay. % input of dDCs transmigrating into the lower chamber with
680 or without macrophages prepared from the skin.

681

682 **Figure 6:** IL-1α upregulates CXCR2 ligands expression in M2-phenotype macrophages to
683 form DC clusters. (**a**) Scores of DC cluster numbers in NT or 24 h after hapten-painted sites
684 in WT, IL-1R-, NALP3-, or caspase 1 (Casp1)-deficient mice (n=4, each). (**b**) Scores of DC
685 cluster numbers in NT or 24 h after hapten-painted sites in isotype control IgG,
686 anti-IL-α antibody, anti-IL-1β antibody, IL-1R antagonist, or pertussis toxin (Ptx)-treated
687 mice (n=4, each). (**c, d**) Ear swelling 24 h after DNFB application (c) and the number (left)
688 and the % frequency (right) of IFN-γ producing $CD8^+$ T cells in the ear 18 h after DNFB
689 application (d) in mice that lack both IL-1α and IL-1β (red) and WT (black) mice (n = 5,
690 each) which were adoptively transferred with DNFB-sensitized T cells. *, $P < 0.05$. (**e**, **f**)
691 Relative amount of *Il1r1* and *Cxcl2* mRNA expression. Quantitative RT-PCR analysis of
692 mRNA obtained from M1 or M2-phenotype macrophages (e), cultured with (+) or without (-)

A Self-archived copy in
Kyoto University Research Information Repository
https://repository.kulib.kyoto-u.ac.jp

693 IL-1α (f) (n=4, each). (**g**) Scores of DC cluster numbers in NT or 24 h after hapten-painted
694 sites in the presence (SB265610) or absence (vehicle) of a CXCR2 inhibitor (n=4, each). *, *P*
695 < 0.05. (**h, i**) Ear swelling 24 h after DNFB application (h) and the number (right) and the %
696 frequency (left) of IFN-γ producing $CD8^+$ T cells 18 h after DNFB application (i) with (red)
697 or without (black) SB265610-treatment (n = 5, each). *, $P < 0.05$.

京都大学 KYOTO UNIVERSITY
A Self-archived copy in
Kyoto University Research Information Repository
https://repository.kulib.kyoto-u.ac.jp
京都大学学術情報リポジトリ KURENAI 紅 Kyoto University Research Information Repository

Figure 1

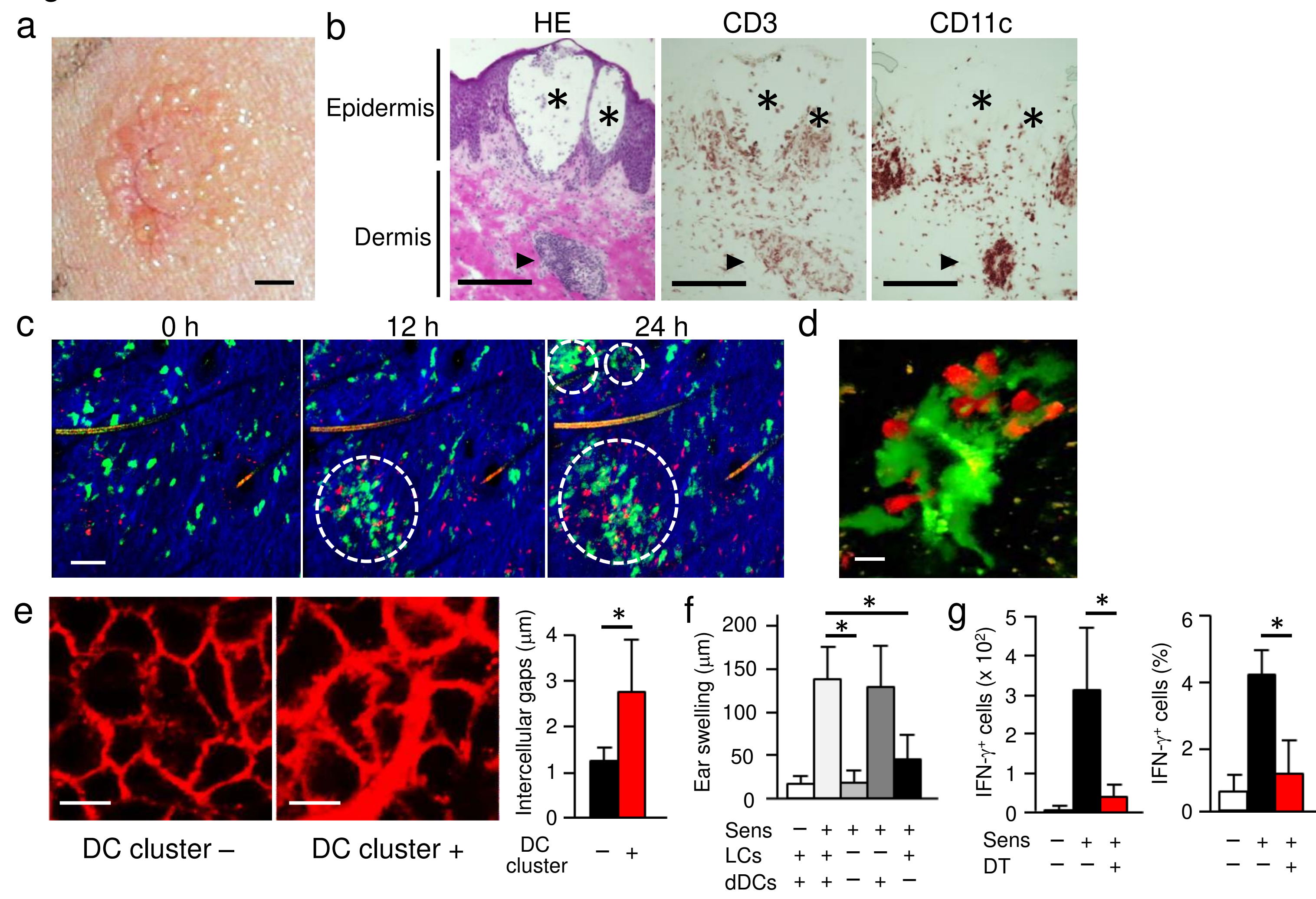

京都大学 KYOTO UNIVERSITY
A Self-archived copy in
Kyoto University Research Information Repository
https://repository.kulib.kyoto-u.ac.jp
京都大学学術情報リポジトリ KURENAI 紅 Kyoto University Research Information Repository

Figure 2

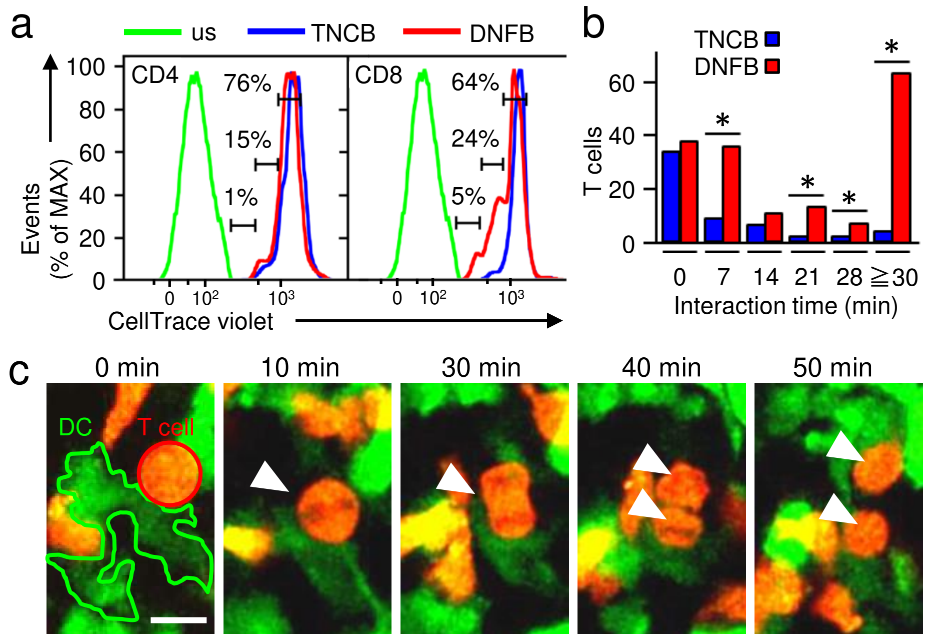

京都大学 KYOTO UNIVERSITY
A Self-archived copy in
Kyoto University Research Information Repository
https://repository.kulib.kyoto-u.ac.jp
京都大学学術情報リポジトリ KURENAI 紅 Kyoto University Research Information Repository

Figure 3

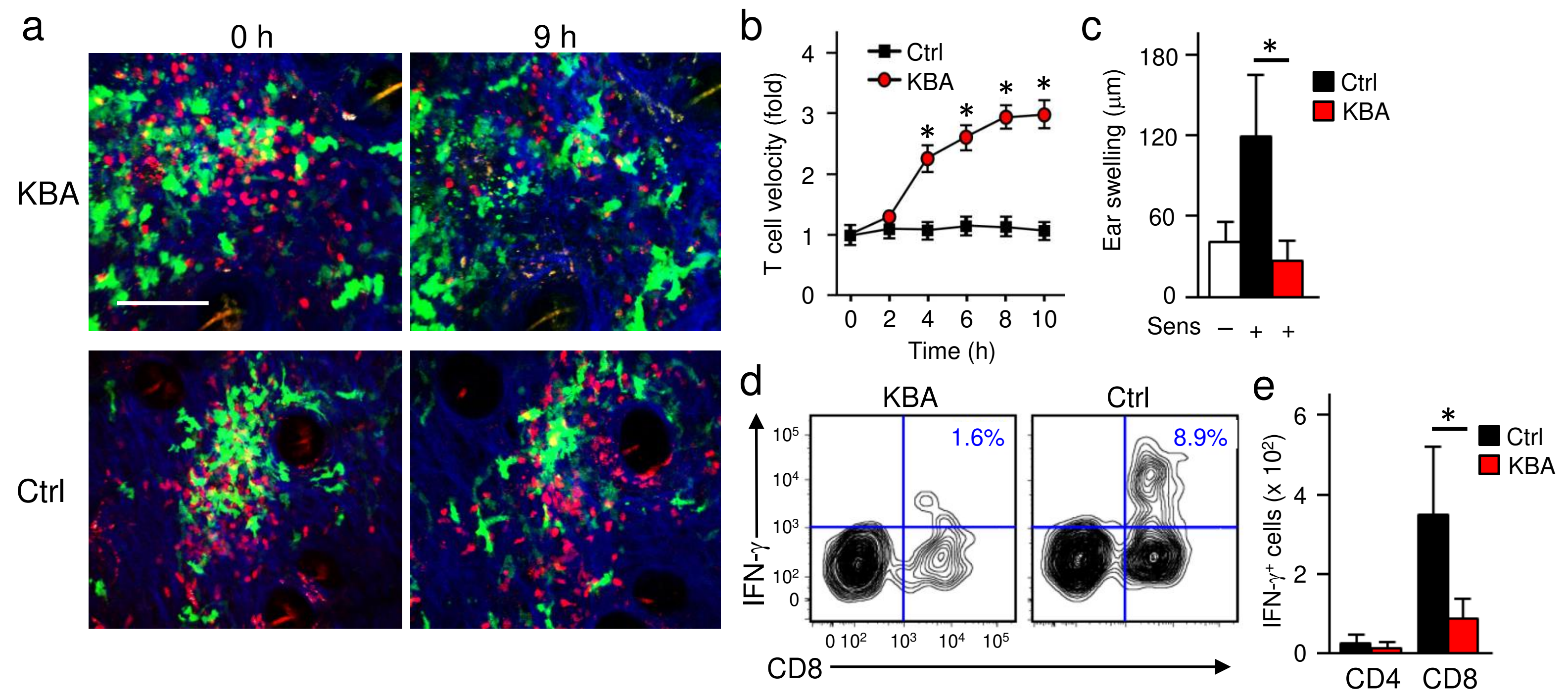

京都大学 KYOTO UNIVERSITY
A Self-archived copy in
Kyoto University Research Information Repository
https://repository.kulib.kyoto-u.ac.jp
京都大学学術情報リポジトリ KURENAI 紅 Kyoto University Research Information Repository

Figure 4

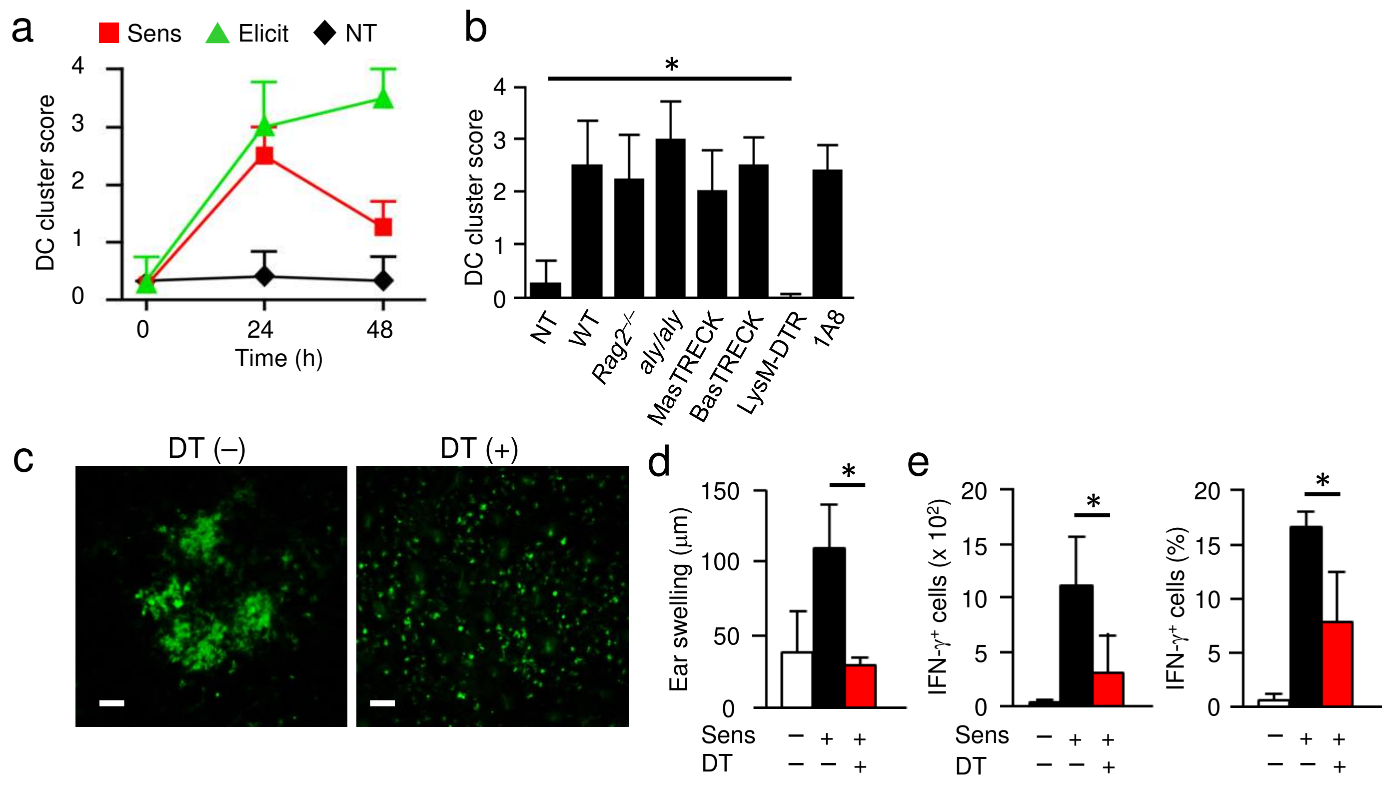

京都大学 KYOTO UNIVERSITY
A Self-archived copy in
Kyoto University Research Information Repository
https://repository.kulib.kyoto-u.ac.jp
京都大学学術情報リポジトリ KURENAI 紅
Kyoto University Research Information Repository

Figure 5

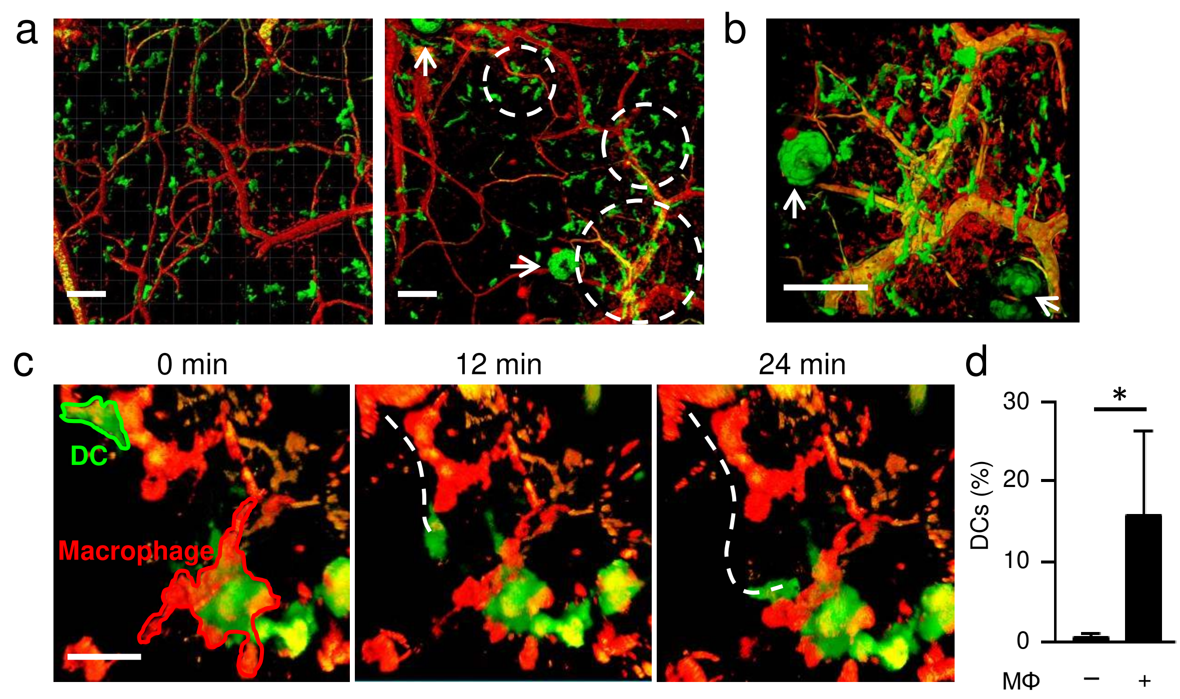

京都大学 KYOTO UNIVERSITY
A Self-archived copy in
Kyoto University Research Information Repository
https://repository.kulib.kyoto-u.ac.jp
京都大学学術情報リポジトリ KURENAI 紅 Kyoto University Research Information Repository

Figure 6

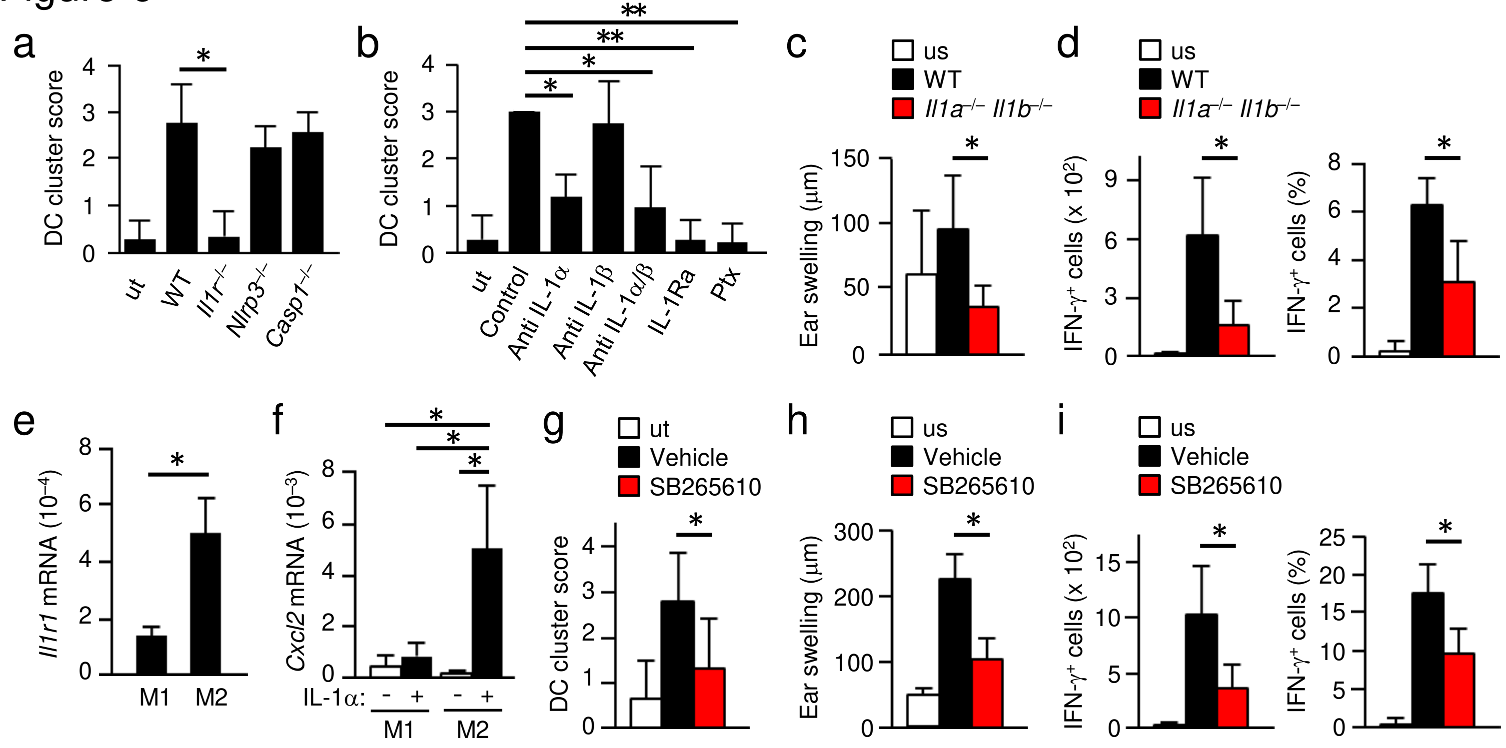

京都大学 KYOTO UNIVERSITY
A Self-archived copy in
Kyoto University Research Information Repository
https://repository.kulib.kyoto-u.ac.jp
京都大学学術情報リポジトリ KURENAI 紅 Kyoto University Research Information Repository

Supplementary Figure 1

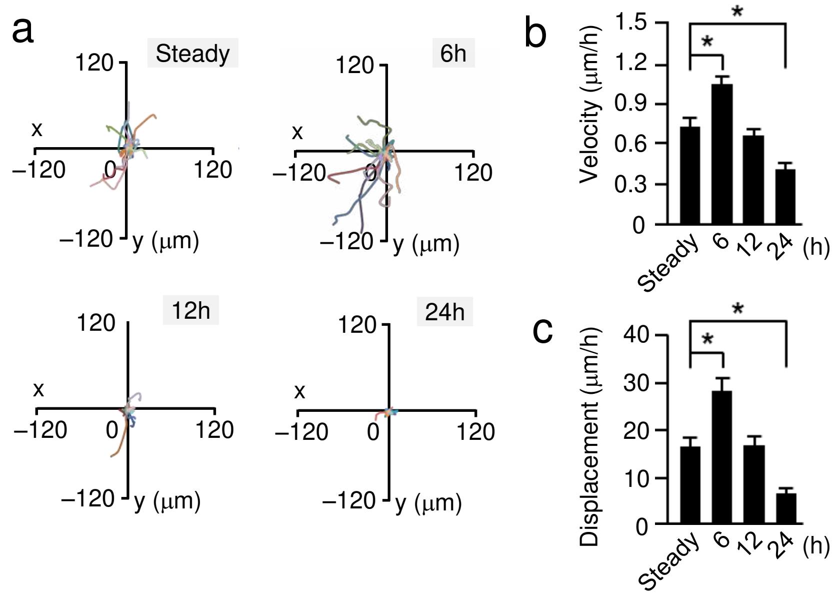

京都大学 KYOTO UNIVERSITY
A Self-archived copy in
Kyoto University Research Information Repository
https://repository.kulib.kyoto-u.ac.jp
京都大学学術情報リポジトリ KURENAI 紅 Kyoto University Research Information Repository

Supplementary Figure 2

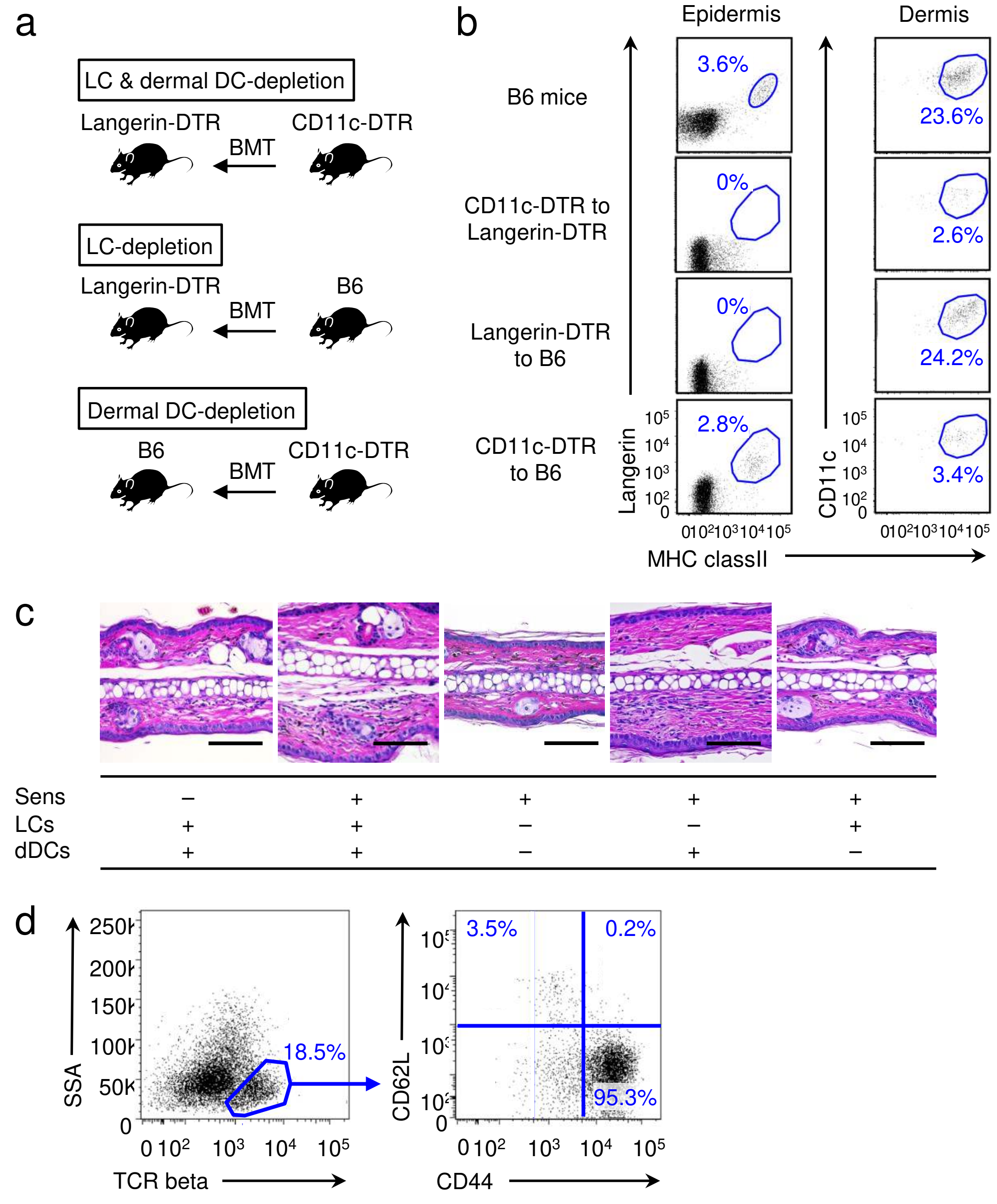

京都大学 KYOTO UNIVERSITY
A Self-archived copy in
Kyoto University Research Information Repository
https://repository.kulib.kyoto-u.ac.jp
京都大学学術情報リポジトリ KURENAI 紅
Kyoto University Research Information Repository

Supplementary Figure 3

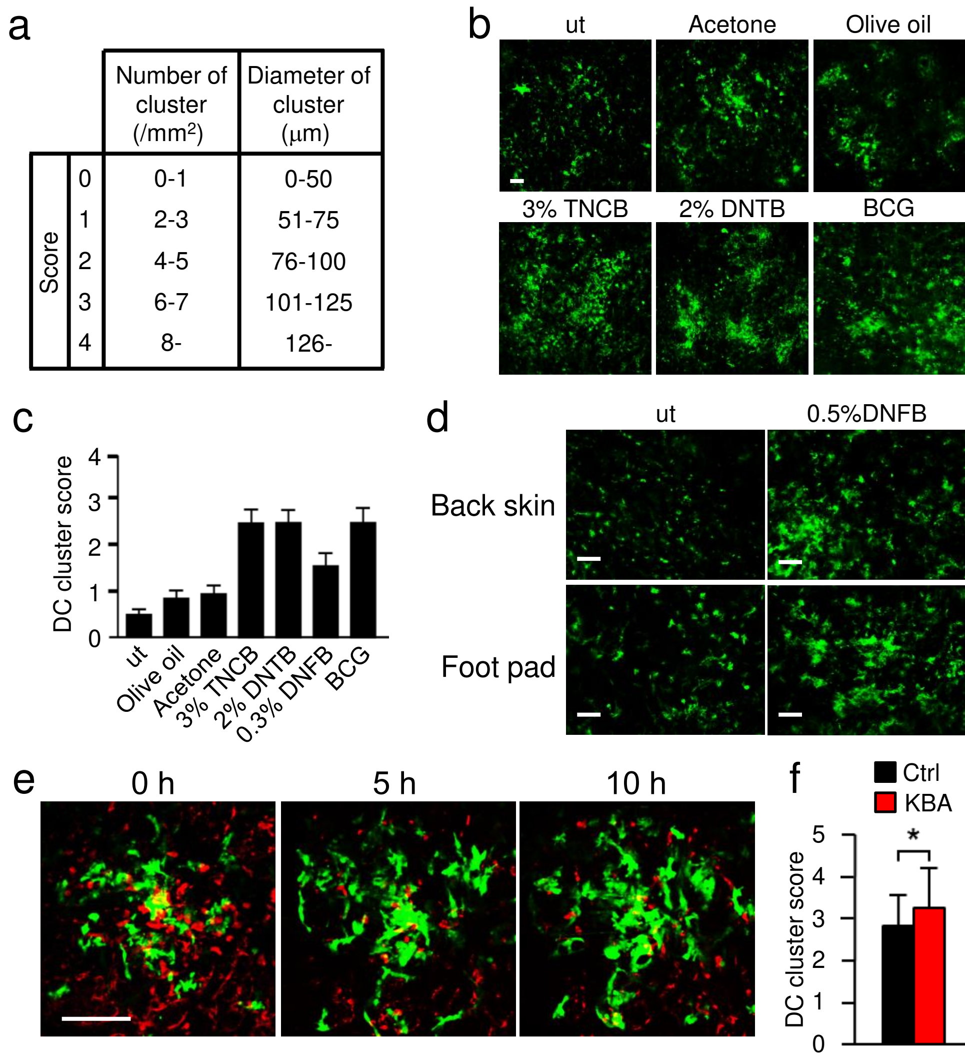

Score	Number of cluster (/mm^2)	Diameter of cluster (μm)
0	0-1	0-50
1	2-3	51-75
2	4-5	76-100
3	6-7	101-125
4	8-	126-

京都大学 KYOTO UNIVERSITY
A Self-archived copy in
Kyoto University Research Information Repository
https://repository.kulib.kyoto-u.ac.jp
京都大学学術情報リポジトリ KURENAI 紅 Kyoto University Research Information Repository

Supplementary Figure 4

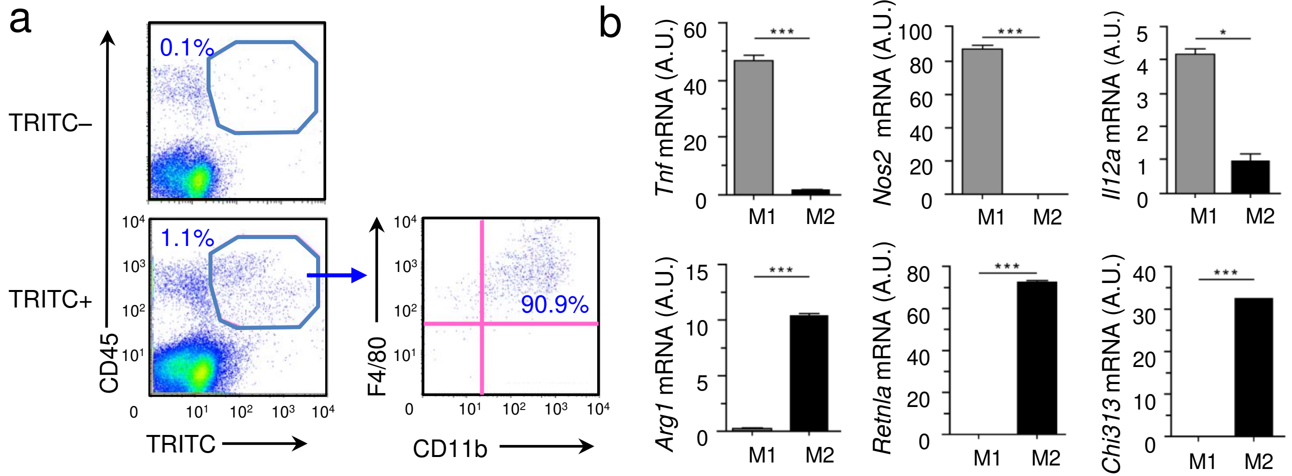

京都大学 KYOTO UNIVERSITY
A Self-archived copy in
Kyoto University Research Information Repository
https://repository.kulib.kyoto-u.ac.jp
京都大学学術情報リポジトリ KURENAI 紅 Kyoto University Research Information Repository

Supplementary Figure 5

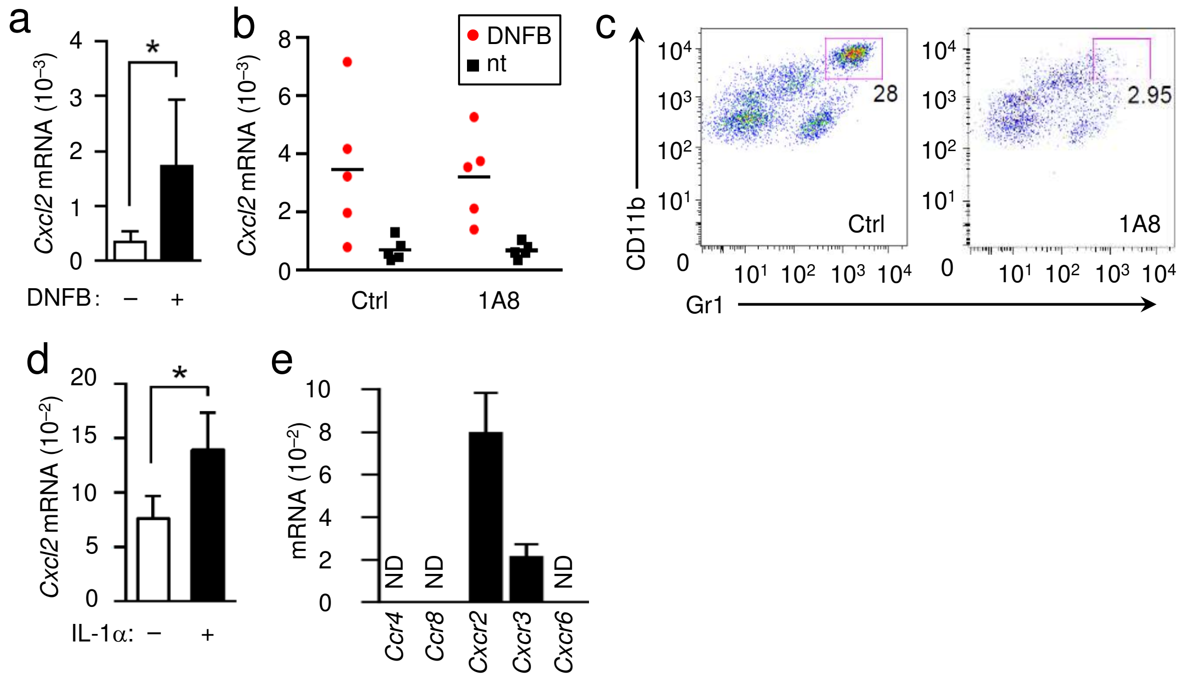

京都大学 KYOTO UNIVERSITY
A Self-archived copy in
Kyoto University Research Information Repository
https://repository.kulib.kyoto-u.ac.jp
京都大学学術情報リポジトリ KURENAI 紅 Kyoto University Research Information Repository

Supplementary Figure 6